Electronic Supplementary Material (ESI) for Physical Chemistry Chemical Physics.

Supplementary Information

Ultrafast Proton Transfer of the Aqueous Phenol Radical Cation

Muhammad Shafiq Bin Mohd Yusof,[1] Hongwei Song,[2] Tushar Debnath,[1] Bethany Lowe,[1] Minghui Yang,[2,3] Zhi-Heng Loh[1,*]

[1] Division of Chemistry and Biological Chemistry, School of Physical and Mathematical Sciences, Nanyang Technological University, 21 Nanyang Link, Singapore 637371, Singapore

[2] State Key Laboratory for Magnetic Resonance and Atomic and Molecular Physics, Wuhan Institute of Physics and Mathematics, Innovation Academy for Precision Measurement Science and Technology, Chinese Academy of Sciences, Wuhan 430071, China

[3] Wuhan National Laboratory for Optoelectronics, Huazhong University of Science and Technology, Wuhan 430071, China

[*] Corresponding author. E-mail: zhiheng@ntu.edu.sg

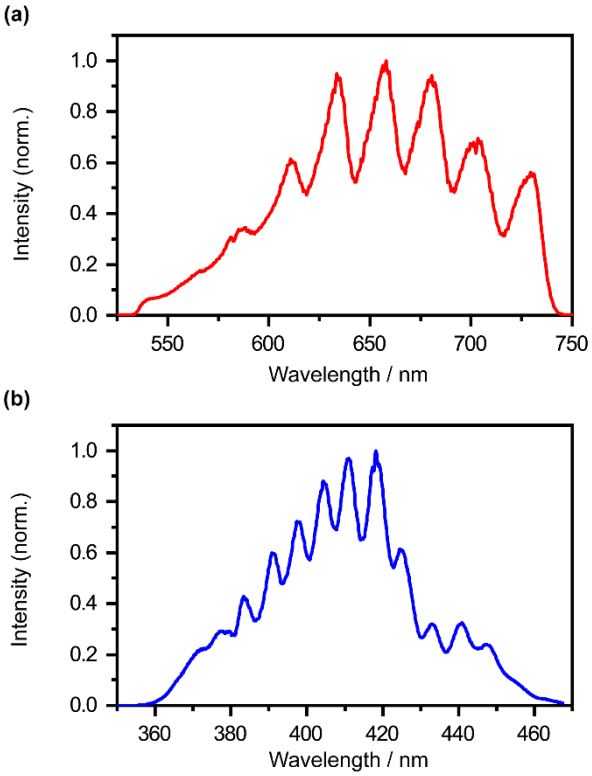

Fig. S1. (a) The visible-NIR ionizing pump spectrum ranges from 520 nm to 750 nm, with a centered wavelength of 636 nm. **(b)** The broadband near-UV probe spectrum ranges from 360 nm to 470 nm.

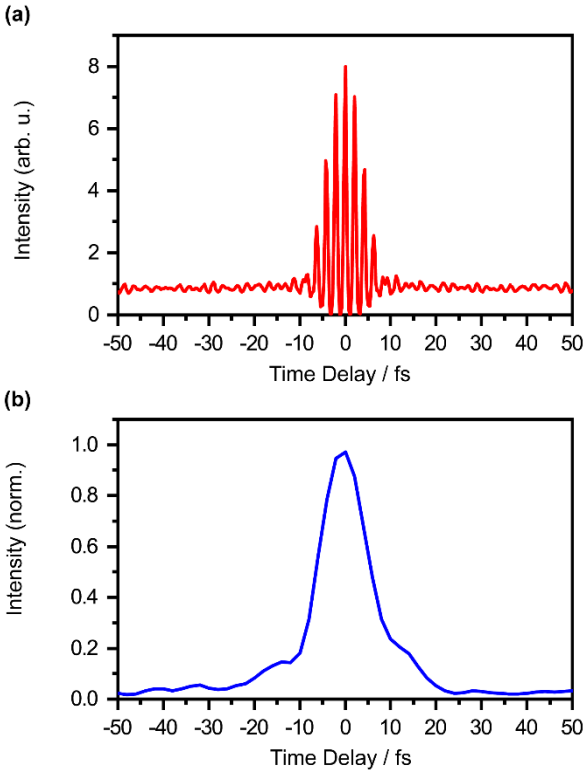

Fig. S2. (a) A second-order interferometric auto-correlation trace of the visible-NIR ionizing pump, measured in a 10-μm-thick, θ = 37.0 deg Type I BBO crystal, reveals a pulse duration with full-width half-maximum (FWHM) of ~ 6.2 fs. **(b)** The visible-NIR pump – near-UV probe cross-correlation, measured *via* difference frequency mixing in a 10- μm-thick, θ = 37.0 deg Type I BBO crystal, reveals a FWHM of 12 fs.

Section S1: Photon-order Measurements for Strong-field Photoionization of Phenol in Aqueous Solution

A power-dependence measurement is performed to determine the photon order of the strong-field photoionization process of phenol in aqueous solution. For an *N*-photon photoionization process, the differential absorption signal, ΔA, scales with intensity of the ionizing pump, I, i.e. $\Delta A \propto I^N$. The photon-order measurements are performed by using the near-UV probe, which measures the absorption of the phenol radical cation at a pump-probe time delay of 1.5 ps. The photon-order measurements are performed in the near-UV region as the phenol radical cation absorbs in the near-UV region. Hence, the absorption signal is proportional to the extent of the photoionization process.

In our study, the ΔA against ionizing pump power spectrum is recorded for aqueous phenol, which is shown in Fig. S3. The ΔA signal is then fitted with the following function:

$$\Delta\Delta A = \alpha I^N/[1 + (I/I_{\mathrm{sat}})^N] \quad (1)$$

where α is the amplitude, N is the photon order and I_{sat} is the saturation intensity. The converged fit when N = 4 yields α = (1.70 ± 0.02) × 10^{-58} cm^2 W^{-1} and I_{sat} = (8.39 ± 0.38) × 10^{13} W cm^{-2}. The value of N indicates that the photoionization of aqueous phenol occurs *via* a four-photon process.

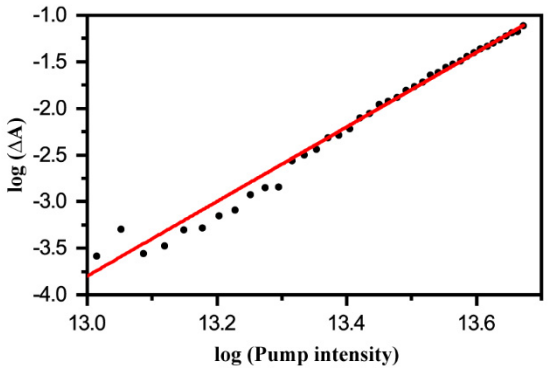

Fig. S3. Photon-order measurement for the strong-field photoionization of the phenol. Log-log plot of ΔA vs. pump intensity reveals a four-photon process for the photoionization of aqueous phenol.

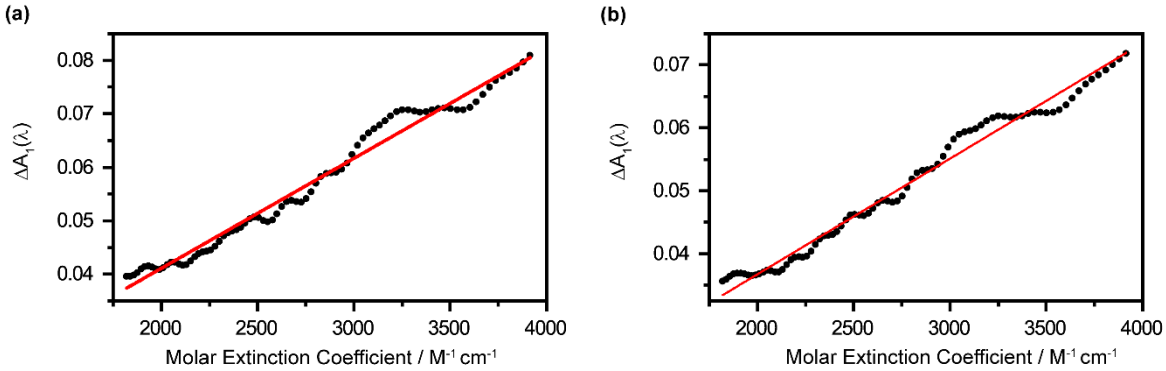

Fig. S4. Plot of ΔA_1 as a function of molar extinction coefficient of hydrated electron, and the linear fit function, in red for **(a)** ionized aqueous phenol and **(b)** ionized liquid water. The gradient of the linear fit function corresponds to the product of the concentration of hydrated electron, c_e and the sample path length, L, which are $(2.056 \pm 0.007) \times 10^{-5}$ M·cm and $(1.838 \pm 0.006) \times 10^{-5}$ M·cm, respectively.

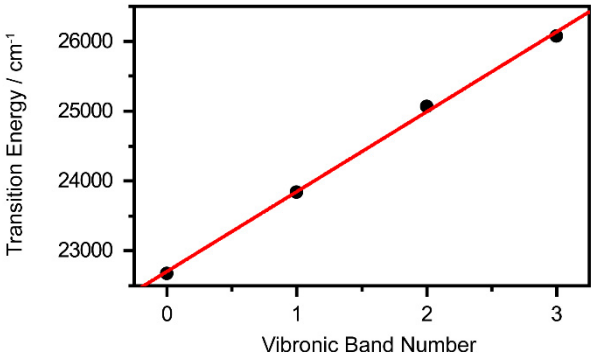

Fig. S5. A linear fit to the transition energies of the vibronic bands reveals a spacing of 1135 ± 34 cm^{-1} for the vibronic progression.

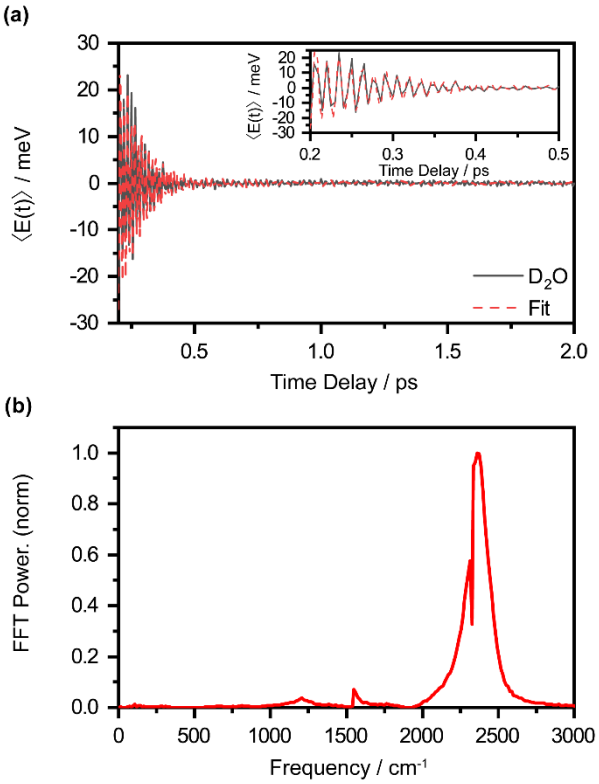

Fig. S6. (a) First-moment time trace, $\langle E(t) \rangle$, of the ionized liquid D_2O. The inset shows the enlarged $\langle E(t) \rangle$ from 0.2 ps to 0.5 ps. **(b)** FFT power spectrum of the first-moment time trace of ionized liquid D_2O. Note that the O_2 and N_2 vibrational frequencies are also observed at 1552 cm^{-1} and 2334 cm^{-1}, respectively.

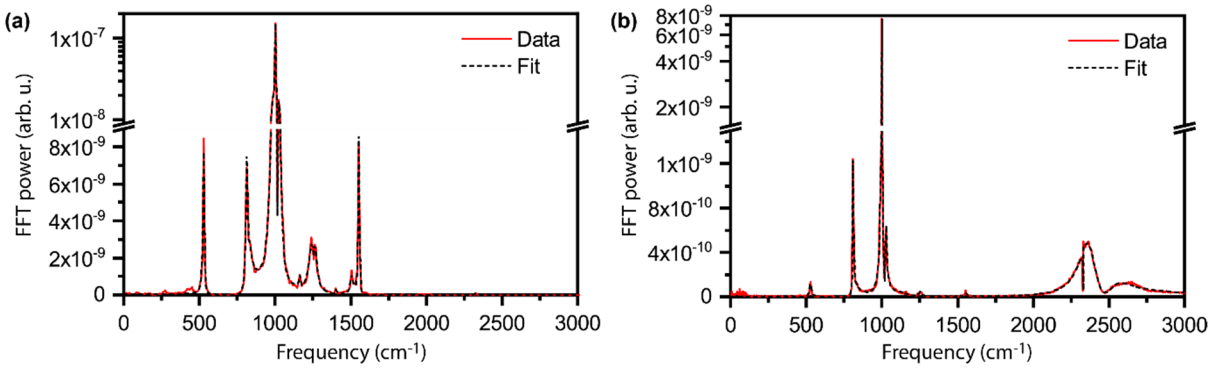

Fig. S7. FFT power spectra of the experimental first-moment time trace and its time-domain fit for ionized **(a)** PhOH and **(b)** PhOD. The good agreement between the experimental data and the fit suggests that the fit parameters obtained from the time-domain fit are reliable.

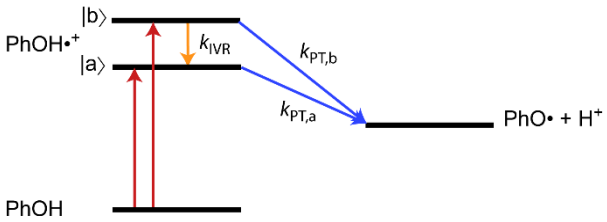

Fig. S8. Schematic energy level diagram of phenol (PhOH), phenol radical cation (PhOH•$^{+}$) and phenoxyl radical (PhO•). States $|a\rangle$ and $|b\rangle$ correspond to the vibrational ground and excited states of the vibrational modes of phenol radical cation with dominant OH or OD character. These vibrational states can undergo depopulation via proton transfer (PT), while the vibrationally excited state can also undergo intramolecular vibrational relaxation (IVR).

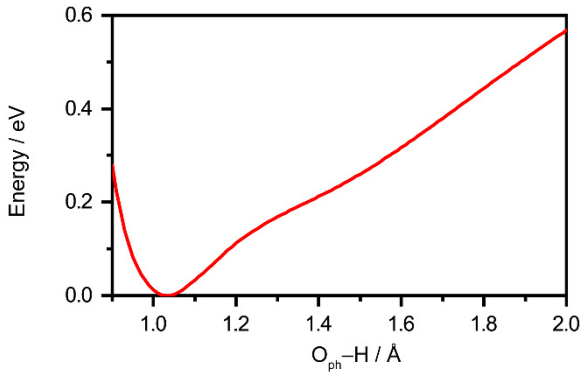

Fig. S9. Potential energy curve as a function of the phenol O_{ph}–H bond length for the microhydrated phenol radical cation, $PhOH^{\bullet+}$-$(H_2O)_3$.

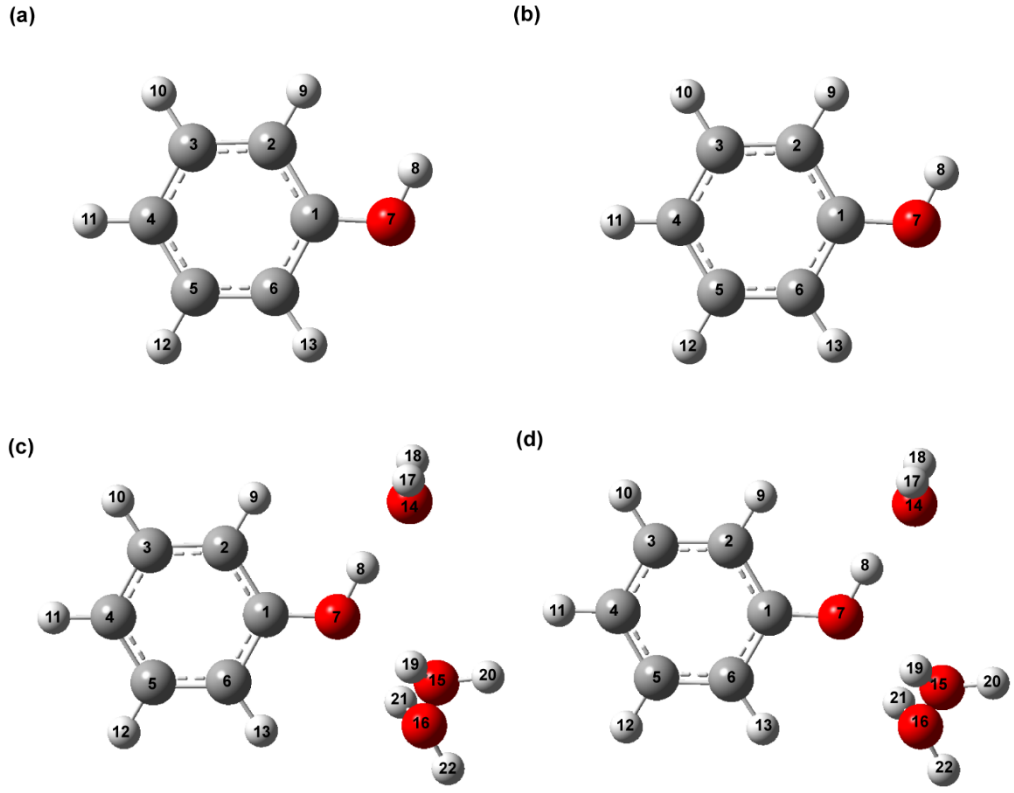

Fig. S10. The equilibrium geometries of the **(a)** phenol radical cation, **(b)** deuterated phenol radical cation, **(c)** microhydrated phenol radical cation, $PhOH^{\bullet+}$-$(H_2O)_3$, and **(d)** microhydrated deuterated phenol radical cation, $PhOD^{\bullet+}$-$(D_2O)_3$, in aqueous solution. The carbon, oxygen and hydrogen atoms are in gray, red and white respectively.

Table S1. Results of time-domain analysis of $\langle E(t) \rangle$ obtained following the ionization of aqueous PhOH. The calculated vibrational frequencies and assignments are those of the microhydrated phenoxyl radical,[1] unless stated otherwise.

Experimental				Calc. Freq. (cm^{-1})	Assignment
Freq. (cm^{-1})	**Amplitude (meV)**	**Damping Time (ps)**	**Phase (π-rad)**		
813 ± 1	0.23 ± 0.02	0.44 ± 0.04	0.67 ± 0.03	818	Ring breath / CCC bend
974 ± 2	0.61 ± 0.09	0.24 ± 0.02	1.14 ± 0.06	988	CCC trig bend
1001 ± 1	0.31 ± 0.01	2.32 ± 0.12	0.59 ± 0.01	1006	Ring breath / CH bend
1027 ± 1	0.14 ± 0.01	1.39 ± 0.20	0.41 ± 0.03	1007	HCCH torsion
1167 ± 3	0.07 ± 0.02	1.35 ± 0.78	1.24 ± 0.01	1164	CH bend
1262 ± 3	0.20 ± 0.11	0.85 ± 0.50	1.04 ± 0.16	1275	CH bend
1246 ± 4	0.52 ± 0.01	0.18 ± 0.02	0.73 ± 0.07	1197	OH wag
1497 ± 5	1.09 ± 0.25	0.16 ± 0.02	1.89 ± 0.06	1414	OH bend
1559 ± 1	0.02 ± 0.01	2.33 ± 0.99	0.40 ± 0.06		O_2
2330 ± 1	0.04 ± 0.01	2.21 ± 0.42	1.97 ± 0.03		N_2

Table S2. Results of time-domain analysis of $\langle E(t) \rangle$ obtained following the ionization of aqueous PhOD. The calculated vibrational frequencies and assignments are those of the microhydrated phenoxyl radical,[1] unless stated otherwise.

Experimental				Calc. Freq. (cm^{-1})	Assignment
Freq. (cm^{-1})	**Amplitude (meV)**	**Damping Time (ps)**	**Phase (π-rad)**		
528 ± 1	0.21 ± 0.01	0.79 ± 0.04	1.51 ± 0.01	541	CCC bend
809 ± 1	0.32 ± 0.01	1.51 ± 0.07	0.18 ± 0.01	818	Ring breath / CCC bend
996 ± 1	0.76 ± 0.03	0.42 ± 0.02	0.37 ± 0.02	988	CCC trig bend
1001 ± 1	0.35 ± 0.01	3.01 ± 0.06	0.23 ± 0.01	1006	Ring breath / CH bend
1026 ± 1	0.22 ± 0.12	1.23 ± 0.11	0.24 ± 0.02	1007	HCCH torsion
1253 ± 2	0.18 ± 0.02	0.48 ± 0.06	0.41 ± 0.04	1295	CC str / CH bend
839 ± 4	0.62 ± 0.10	0.14 ± 0.02	1.58 ± 0.05	870	OD Wag
1166 ± 6	2.55 ± 0.46	0.07 ± 0.01	0.69 ± 0.06	1170	OD Bend
2373 ± 1	21.87 ± 0.88	0.07 ± 0.01	1.86 ± 0.02	2401, 2489	OD Stretch from D_2O*
2498 ± 3	19.65 ± 1.65	0.06 ± 0.01	1.66 ± 0.02		
1553 ± 1	0.15 ± 0.01	0.54 ± 0.06	1.10 ± 0.03		O_2
2330 ± 1	0.07 ± 0.01	5.52 ± 0.40	1.30 ± 0.01		N_2

*The vibrational frequency of O–D stretching of D_2O is from ref. 2.

Table S3. Density functional theory (DFT)-calculated vibrational frequencies of the isolated and microhydrated phenol radical cation, $PhOH^{\bullet+}$-$(H_2O)_3$, and deuterated phenol (phenol-OD) radical cation, $PhOD^{\bullet+}$-$(D_2O)_3$, embedded in a polarizable continuum (PCM). The assignment of atoms and vibrational modes are based on the equilibrium geometries of the phenol radical cation and the microhydrated phenol radical cation, as shown in Fig. S10.

	Phenol Radical Cation Calc. Freq. (cm^{-1})		**Phenol-OD Radical Cation Calc. Freq. (cm^{-1})**		**Assignment**
	Isolated	**Microhydrated**	**Isolated**	**Microhydrated**	
1	396	475	374	457	CO Bend
2	524	534	519	528	CCC Bend
3	572	578	568	576	CCC Bend
4	818	821	808	813	Ring Breath / CCC Bend
5	990	995	989	995	CCC Trigonal Bend
6	995	999	995	999	CH Bend / Ring Breath
7	1089	1108	1103	1112	CH Bend / CC Stretch
8	1149	1414	922	1014	OH (OD) Bend*
9	1186	1201	1187	1202	CH Bend
10	1195	1275	1166	1334	CH Bend
11	1356	1379	1331	1384	CH Bend
12	1384	1396	1378	1395	CC Stretch
13	1396	1170	1390	1112	CC Stretch
14	1450	1468	1429	1435	CC Stretch
15	1491	1508	1486	1501	CO Stretch
16	1539	1544	1538	1543	CC Stretch
17	1653	1653	1652	1651	CC Stretch
18	3188	3213	3188	3213	CH Stretch
19	3206	3203	3206	3203	CH Stretch

20	3214	3209	3214	3209	CH Stretch
21	3220	3219	3220	3219	CH Stretch
22	3226	3223	3226	3223	CH Stretch
23	3710	2593	2701	1909	OH (OD) Stretch*
24	182	192	178	192	Ring Deformation
25	362	372	356	379	Ring Twist
26	432	439	425	450	Ring Boat
27	601	1197	469	870	OH (OD) Wag*
28	611	634	609	633	CH Wag
29	783	813	780	813	CH Wag / Ring Boat
30	799	796	791	789	CH Wag
31	945	958	940	958	CH Wag / Ring Boat
32	997	1017	995	1017	HCCH Torsion
33	1007	1012	1006	1012	HCCH Torsion

Note that modes 1 – 23 have A’ symmetry and modes 24 – 33 have A’’ symmetry.

References

1. T. Debnath, M. S. B. Mohd Yusof, P. J. Low and Z.-H. Loh, *Nat. Commun.*, 2019, **10**, 2944.
2. S. R. Pattenaude, L. M. Streacker and D. Ben-Amotz, *J. Raman Spectrosc.*, 2018, **49**, 1860-1866.